Numerical Investigation of Wind-Induced Interference in a Random Urban Array

Ahmad Faiz Mohammad[1], Sheikh Ahmad Zaki[1]*,
Mohamed Sukri Mat Ali[1], Fitri Yakub[1]
Malaysia-Japan International Institute of Technology,
Universiti Teknologi Malaysia, Kuala Lumpur, Malaysia

Aya Hagishima
Interdisciplinary Graduate School of Engineering
Sciences, Kyushu University, Fukuoka, Japan

*sheikh.kl@utm.my

ABSTRACT

The presence of surrounding obstacles influences wind velocity and pressure distributions in a building cluster. Computational fluid dynamics (CFD) modelling approach namely Large Eddy Simulation (LES) was performed in simulating the wind flow in a random urban array comprised of vertically random building clusters. Wind pressure distribution was analysed using two parameters: (a) reference pressure coefficient ($C_{p_{ref}}$) based on the pressure difference between an arbitrary and free-stream points and (b) wind pressure coefficient ΔC_p based on the pressure difference between windward and leeward building surfaces. The contour plots of $C_{p_{ref}}$ surrounding the tallest building showed the wind-induced interference decreased with height for two wind directions tested (0° and 180°), indicated by the increasing $C_{p_{ref}}$ values. The $C_{p_{ref}}$ distribution along the horizontal sections of the same building also showed its values increased with height. Finally, the local interference effects were parameterized in each building cluster containing a target building for which the target ΔC_p (henceforth $\Delta C_{p_{target}}$) and height (h_{target}) were determined. Current results showed that $\Delta \frac{C_{p_{target}}}{\Delta C_{p_{ave}}}$ is almost linearly proportional with h_{target}/h_{ave}. These findings can be used to assess the wind-induced interference effects on natural ventilation potential particularly in random arrays.

Introduction

Impacts of interfering obstacles on the wind flow and pressure distribution surrounding a target building are considered in many applications such as wind-induced ventilation [1 - 4], wind loading on urban structures [5 - 7], urban aerodynamic parameters [8 - 11], and pollutant dispersion [12, 13]. Such impacts are associated with wind flow properties like velocity and pressure before and after which the interfering obstacles are present. This can be termed as wind-induced interference effects [5, 6].

Wind-induced interference effects are prevalent particularly in dense urban areas. Natural wind paths are obstructed and deflected upon the interaction with building surfaces, often resulting in reduced velocity and enhanced turbulence [1, 3]. This is most critical in urban canopy layer which typically lies below the average building height [14, 15]. Oke [16] identified three distinctive flow regimes within urban canopy layer based on the height-to-width ratio (h/w) of street canyon. These flow regimes are isolated roughness flow ($h/w \leq 0.3$), wake interference flow ($0.3 < h/w \leq 0.7$), and skimming flow ($h/w \geq 0.7$). The interference effects exist when the deflected flow from the upwind building overlaps with the deflected flow (recirculation) caused by the downwind building. These effects magnify as the separation distance w between the two buildings reduces. Such observations are specific to the interfering buildings of the same height (i.e. uniform building array). Nevertheless, the identified flow regimes lay out a basis for which the interference effects in non-uniform (or random) arrays have been subsequently studied [8].

The interest in investigating wind-induced interference effects particularly of urban topologies has developed over time. One of the notable studies is Khanduri et al. [5] that reviewed a number of past studies focusing on wind loading. They highlighted that the interference between two similar buildings, analysed using the wind force exerted on a target building under the influence of an upstream interfering building, can either increase or decrease depending on the incident wind angle and the separation distance between the two buildings. In fact, Desai et al. [7] showed that the interference is minimal when the incident wind angle coincides with the upstream building position, even when the separation distance varies.

However, local geometric effects within an urban array (or a cluster of buildings) have not been properly parameterized unlike for the configuration of two buildings. Urban arrays are typically represented by global parameters such as packing density (λ_p) i.e. the fraction of ground surface area covered by buildings [2, 4] and frontal area density (λ_f) i.e. the ratio of frontal

building area to the ground surface area [8, 17]. However, the relationships between such parameters and various urban processes such as wind-induced ventilation [2], pedestrian wind comfort [17], and aerodynamic parameters [8 - 11] have been well documented.

The analysis target of this study is the wind pressure distribution within an urban array. Zaki et al. [2] analysed the wind pressure coefficients (ΔC_p) of clustered buildings with varying packing densities in estimating wind-induced ventilation for uniform building arrays. A higher ΔC_p indicates a better ventilation potential, which was obtained for low λ_p in which the interference effects are minimal. However, the use of random arrays has not been documented for studying ΔC_p, although Xie et al. [18] used a random array to investigate the relationship between the building aspect ratio (height-to-width ratio) and pressure drag.

Therefore, the aim of this study is the investigation of interference effects on wind pressure distribution in a random building array. The random building array is based on the wind tunnel study of Zaki et al. [9] and comprised of several building clusters that will be explained later. This study performs computational fluid dynamics (CFD) simulations using OpenFOAM® software. Computational setting and model configuration will be explained in the next sections.

Numerical Procedure

Computational setting

Large-eddy simulation (LES) has been applied for resolving complex turbulent flows particularly in urban-related studies such as Razak et al. [17] and Xie et al. [17]. LES is known for its capability to estimate mean and turbulent flow scales more accurately than Reynolds-averaged Navier-Stokes (RANS) although it has been known to be less accurate than direct numerical simulations (DNS) [19]. Since DNS generally requires a high computing capacity to resolve turbulent scales with high accuracy, LES is the most viable option considering our current computational resources. Smagorinsky sub-grid scale (SGS) model was used in OpenFOAM® with Smagorinsky constant C_s of 0.1 [17, 18].

OpenFOAM® uses the finite volume method for the discretization of the governing equations; the second order Gauss linear scheme was applied for spatial discretization and the second order backward scheme was applied for time integration, both of which are the minimal requirements for accurate flow simulation with LES [19]. PIMPLE algorithm was used since the flow simulation required a transient solution. The number of correctors applied was three so that for each time step, the iteration was repeated three times to achieve the final residual set to 1×10^{-5} particularly for all velocity components (streamwise, spanwise, and vertical) and pressure. The

simulation convergence was achieved through the default setting of the PIMPLE algorithm.

Model configuration

The urban model used in this study is the random array that is made up of vertically random, square-based buildings. Two simulation cases i.e. R17A and R17B were set up using the random array under two wind directions i.e. *A* (0º) and *B* (180º), as shown in Figure 1. The buildings are represented with notations (b1 to b9) for their individual heights, as detailed in Table 1. The packing density of the urban models λ_p is 0.17. The domain height is $15h$ that is approximately four times the height of the tallest building ($3.76h$) where h is the standard height scale equal to 25 mm. This selection was made based on the previous CFD studies [17, 18] which found that the dependency of mean turbulent flows within urban canopy layer was weak against the domain height. In addition, the average height and standard deviation of the simulation model are $1.5h$ and 1.15, respectively, based on the experimental study of Zaki et al. [9].

Figure 1: Plan view of the model where the notations b1 to b9 represent building heights
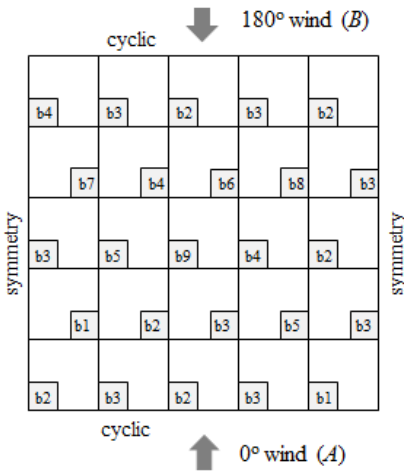
Table 1: Individual building height (h is 25 mm)

Building	Height
b1	0.36h
b2	0.84h
b3	1.32h
b4	1.50h
b5	2.00h
b6	2.64h
b7	3.00h
b8	3.32h
b9	3.76h

The boundary conditions applied to the computational domain are as follows:

i. Cyclic condition in the streamwise boundaries to simulate an infinite domain of continuous flow;

ii. Symmetry condition in the lateral boundaries to simulate a similar flow condition on the right and left sides of the domain since the random array is unsymmetrical;

iii. Free-slip condition in the top boundary to simulate a free atmosphere;

iv. No-slip condition (with wall function based on log law) on the wall surfaces (buildings and domain floor) to develop a boundary layer effect.

In addition, the internal flow is driven by pressure gradient force [17], and its equation is shown below:

$$\partial P / \partial x = \rho u_*^2 / L_z \tag{1}$$

In Equation (1), ρ is the air density at sea level, u_* is friction velocity, and L_z is the domain height.

Sensitivity and Validation Studies

To show the convergence of the simulation results obtained using the LES, the statistical analysis was performed for different averaging periods. The eddy turnover time T is determined as h_{ave}/u_* [17, 18] where h_{ave} is the average building height and u_* is the friction velocity. The normalized statistical moments i.e. U/U_{ref}, σ/U, u'^3/σ^3, and u'^4/σ^4 (where U/U_{ref} is the normalized streamwise velocity, σ is standard deviation, u'^3 is skewness, and u'^4 is kurtosis) were plotted (at an arbitrary point in the computational domain) for averaging periods of $200T$, $400T$, and $600T$. Since the results for both cases (R17A and R17B) are nearly identical, only those of one LES case (i.e. R17B) are shown in Figure 2. The plots show that the simulation convergence is achieved at $400T$, which is consistent with the previous LES studies of turbulent, incompressible flows [17, 18]. Moreover, $200T$ is inadequate for the velocity to converge particularly for the random array used in this study.

Validation with the previous wind tunnel data [9] is also crucial to ensure the accuracy and consistency of the LES results. For this purpose, mean streamwise velocities (time-averaged for $400T$) were spatially averaged across the domain for three different resolutions i.e. 36, 64, and 100 points as shown in Figure 3. The results were normalized with the reference velocity U_{ref} of approximately 10 m/s taken at the reference height of $z/h = 14$ at which the effect of surface roughness is predominantly absent. The normalized mean velocity profiles for both cases i.e. R17A and R17B are shown in Figure 4, along with the wind tunnel (WT) result of Zaki et al. [9].

In Figure 4, the LES velocity profiles with 100 sampling points agree well with the WT profile from z/h of 6 to 14, while the profiles with the less sampling points i.e. 64 and 36 deviate from the WT profile in the same region. However, relative to WT, all sampling points show underestimation

of velocity profiles in the range of $z/h < 6$ primarily due to the insufficiency of grid resolution within this height where the surface roughness effects on the mean velocity might still be significant. The maximum standard error is approximately 0.03 (at $z/h = 2.5$), which is only about 8% of the wind tunnel value at the same height. Nevertheless, this may not have substantial effects on the analysis of wind pressure coefficients of the buildings since the reference velocity was taken at the free-stream height of $z/h = 14$ where the discrepancy of the velocity profiles between the wind tunnel experiment [9] and the present study is negligible.
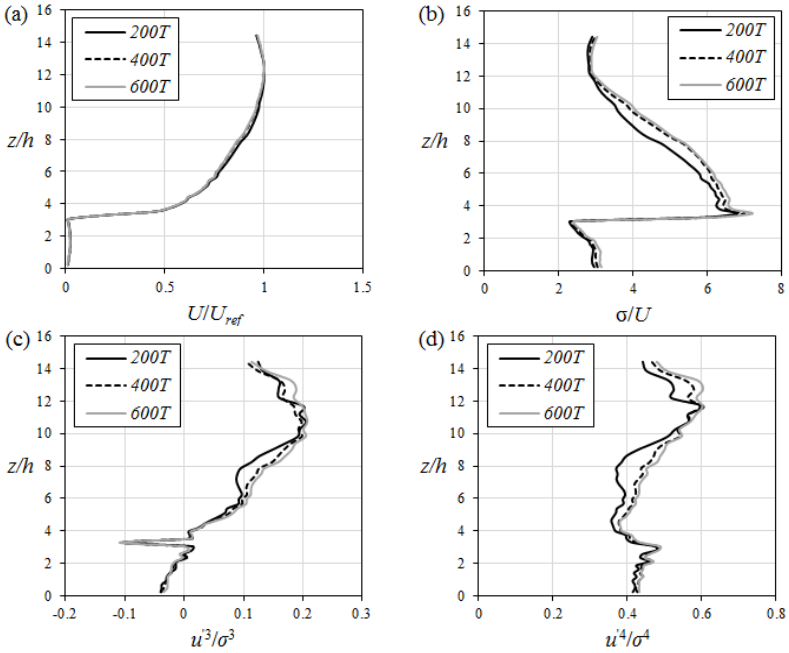
Figure 2: Normalized statistical moments for different averaging periods (a) U/U_{ref} (b) σ/U (c) u'^3/σ^3 (d) u'^4/σ^4
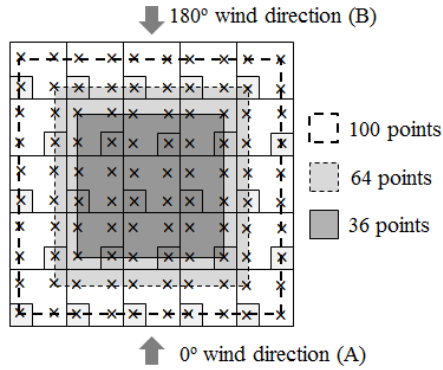
Figure 3: Spatial resolutions for mean velocity sampling where '×' is the sampling point
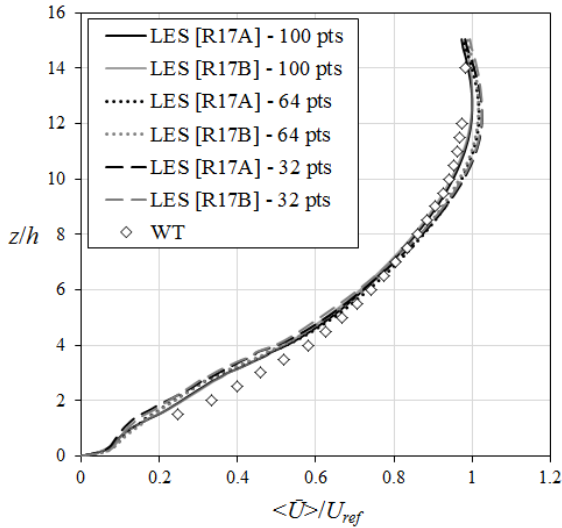
Figure 4: Normalized mean streamwise velocity profiles where WT represents the wind tunnel data of Zaki et al. [9]

Result and Discussion

Mean pressure distribution

In this discussion, the interference effects within a cluster of buildings were investigated for two wind directions i.e. 0° (R17A) and 180° (R17B). The

cluster of buildings within the spatial range of $4h$ to $9.5h$ in both streamwise and spanwise directions was analysed for both cases. The range was selected to include the tallest building i.e. b9 which is located at the centre of the random array. This makes b9 an ideal target for wind-induced interference in both wind directions. The reference of mean pressure coefficient $C_{p_{ref}}$ based on the reference pressure was determined as follows:

$$C_{p_{ref}} = \left(p - p_{ref} \right) / \left(0.5 \rho U_{ref}^2 \right) \tag{2}$$

where p is pressure and p_{ref} is the reference pressure taken at the reference height of $15h$. The $C_{p_{ref}}$ contour plots are shown in Figures 5 to 8. For each case, the heights selected are $0.5h$, $1.0h$, $1.5h$, and $2.0h$ to investigate the varying interference effects with height due to the surrounding buildings. The normalized streamwise velocity U/U_{ref} is also shown at each height as it can be related to understanding the interference effects between the clustered buildings.

In addition, the pressure distributions of b9 do not undergo significant changes from $z/h = 0.5$ (shown in Figure 5) to 1.0 (shown in Figure 6), indicating that the effects of surrounding buildings (particularly b2 and b3) are negligible. This is due to the large separation between the clustered buildings; b9 might be more prone to the interference effects if the packing density increases. Furthermore, for R17B where buildings b2 and b3 are in the downwind region, their impacts on the upwind buildings are nearly absent. Although U/U_{ref} increases from 0.09 (at $z/h = 0.5$) to 0.12 (at $z/h = 1.0$), the $C_{p_{ref}}$ distribution patterns observed particularly surrounding the buildings in the middle i.e. b9, b5, and b4 are almost similar.

As height increases from $1.5h$ (in Figure 7) to $2.0h$ (in Figure 8), U/U_{ref} also increases from 0.20 (at $z/h = 1.5$) to 0.25 (at $z/h = 2.0$). This leads to the increase of $C_{p_{ref}}$ values particularly on the windward side of b9 in both cases. Moreover, the interference from buildings b2 and b3 completely disappears at these heights, while the interference from b4 only disappears at $z/h = 2.0$. In fact, by comparison with the previous results discussed at lower heights, this is where the wind-induced interference effects are minimal. This is further discussed in the next section.
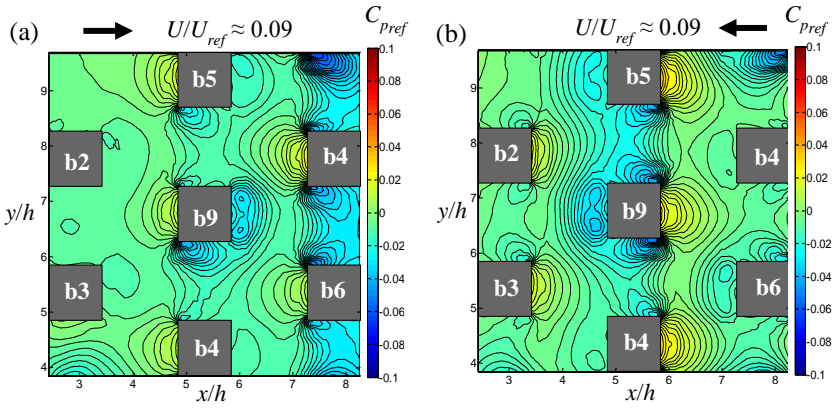
Figure 5: $C_{p_{ref}}$ contour at $z/h = 0.5$ for (a) R17A and (b) R17B where the arrow represents the wind direction
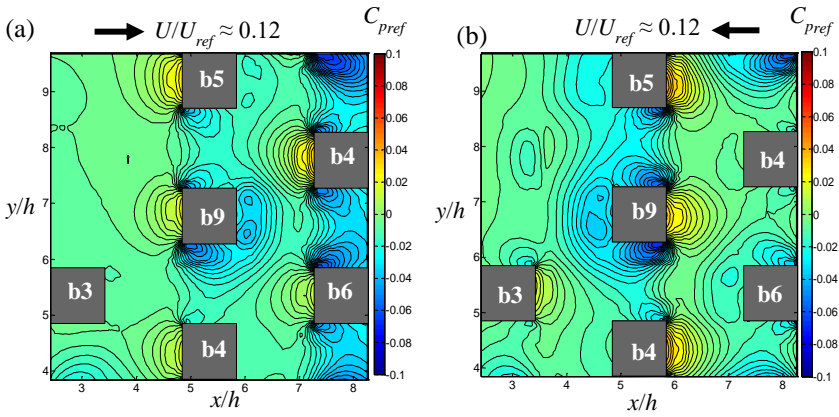
Figure 6: $C_{p_{ref}}$ contour at $z/h = 1.0$ for (a) R17A and (b) R17B where the arrow represents the wind direction
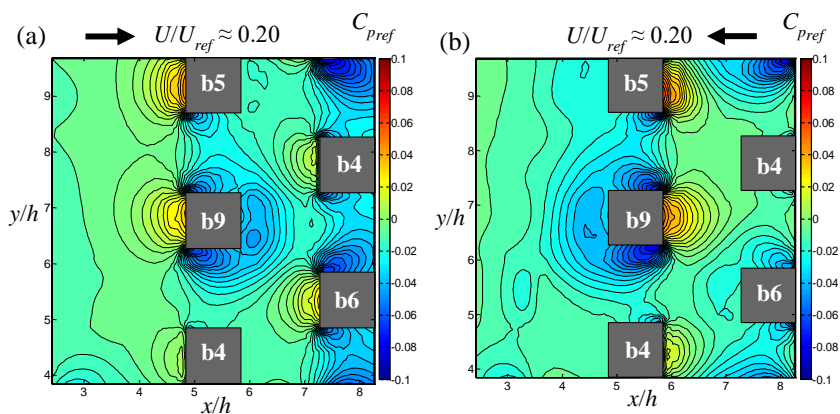
Figure 7: $C_{p_{ref}}$ contour at $z/h = 1.5$ for (a) R17A and (b) R17B where the arrow represents the wind direction
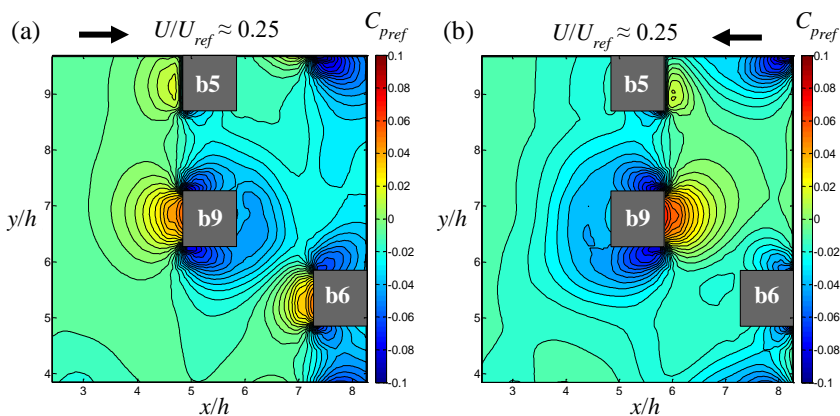
Figure 8: $C_{p_{ref}}$ contour at $z/h = 2.0$ for (a) R17A and (b) R17B where the arrow represents the wind direction

Surface pressure profile

In this discussion, $C_{p_{ref}}$ is plotted along the horizontal sections around the building at four heights i.e. $z/h = 0.5$, 1.0, 1.5, and 2.0. The results are normalized by the maximum $C_{p_{ref}}$, and shown in Figures 9 (a) and (b) for R17A and R17B, respectively. The simulation results are compared with the

wind tunnel result of Kim et al. [20] for the uniform cube array of λ_p= 0.16, and only one horizontal section i.e. at the half of the cube was taken in their study.

From these figures, the normalized $C_{p_{ref}}$ varies with point location x/h and normalized height z/h. Both cases i.e. R17A and R17B show that the normalized $C_{p_{ref}}$ at $z/h = 2.0$ is almost equal to WT [20], particularly on the windward side (region 0 to 1). This suggests that at $z/h = 2.0$, the surrounding interference has the least impact on the building surface pressure, as opposed to lower heights which are more prone to the surrounding obstacles.

(a)

(b)
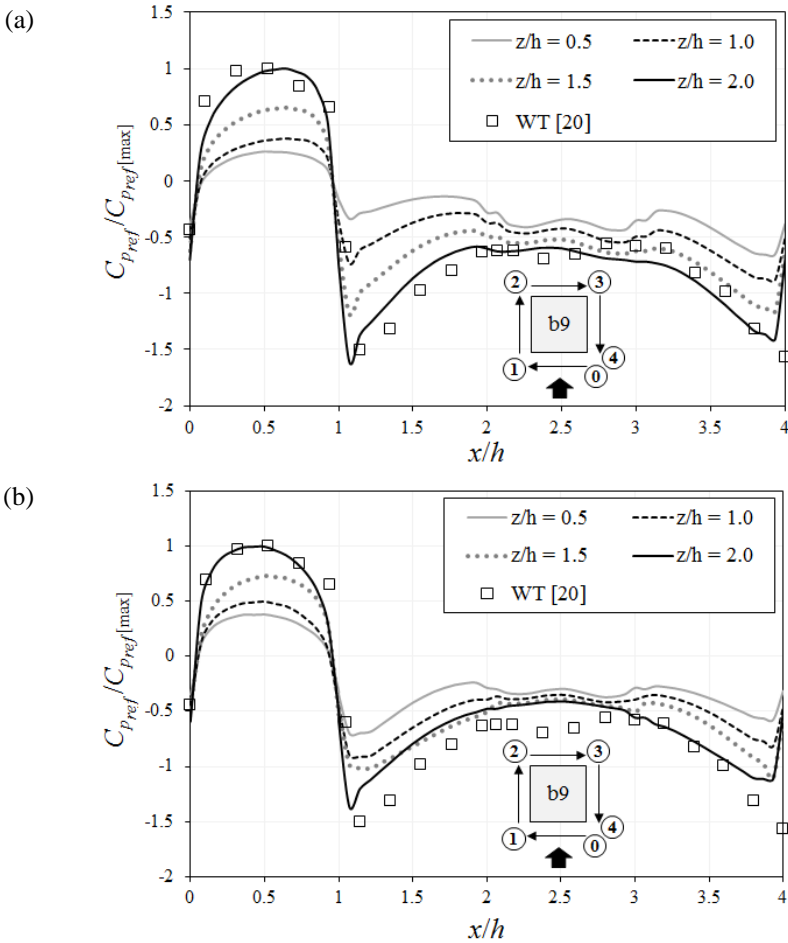
Figure 9: Normalized $C_{p_{ref}}$ at horizontal sections for (a) R17A and (b) R17B where WT [20] is the wind tunnel result of Kim et al. [20]; 0, 1, 2, 3, and 4 refer to the regions along the building horizontal section

Influence of surrounding interference

This next analysis considers the pressure drag contribution of each building in the random array under two wind directions i.e. 0° and 180°. The pressure drag, which is based on the pressure difference between the windward and leeward building surfaces, is non-dimensionalised as the wind pressure coefficient ΔC_p and determined as follows:

$$\Delta C_p = (p_w - p_l) / (0.5 \rho U_{ref}^2) \tag{3}$$

In the equation above, p_w and p_l are the windward and leeward building surface pressures. $\Delta C_{p_{target}}$ represents the ΔC_p of a target building. Each target building is surrounded within a cluster of 6 or more interfering buildings. This is illustrated in Figure 10 below.
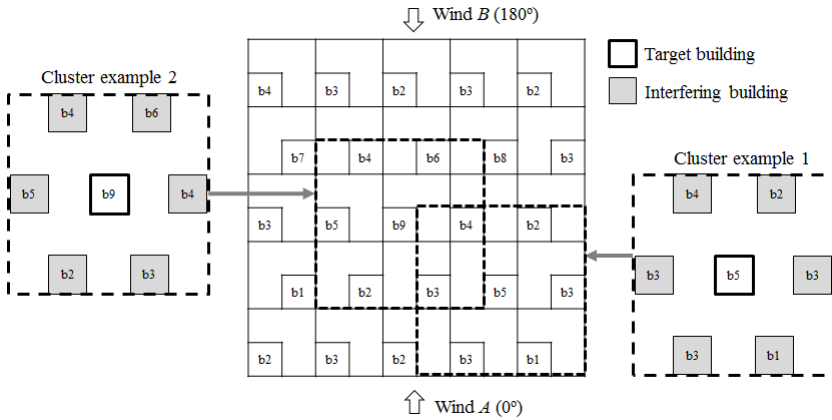
Figure 10: Illustrations of building clusters containing target and interfering buildings

From the illustration above, a total of 25 building clusters (equal to the number of target buildings) are sampled. For each building cluster, $\Delta C_{p_{ave}}$ is determined by averaging the ΔC_p of clustered buildings (both target and interfering buildings). Additionally, the average height of each cluster h_{ave} is also determined. The results of $\Delta C_{p_{target}}$ normalized by $\Delta C_{p_{ave}}$ are plotted

against h_{target} normalized by h_{ave} for all clusters in each case i.e. R17A and R17B, and are shown in Figure 11.
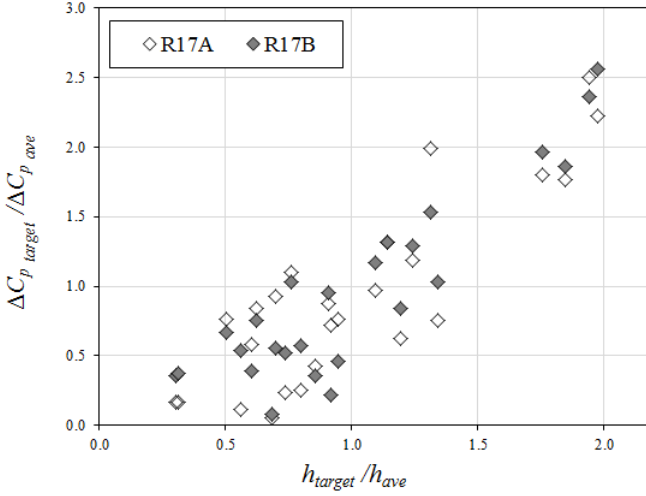
Figure 11: Distribution of the normalized $\Delta C_{p_{target}}$ for all target buildings of all clusters in R17A and R17B

The correlation coefficients between $\Delta C_{p_{target}}/\Delta C_{p_{ave}}$ and h_{target}/h_{ave} of both simulation data are approximately 0.86 and 0.90 for R17A and R17B, respectively. Both values indicate strong positive correlations for the two wind directions studied. In addition, the discrepancies between the values measured for both sets of simulation data are due to the wind direction. Our findings also show that the target building in the random staggered array is considerably affected by the surrounding interference. The linear equation derived from the distributions of both cases is shown in Equation (4) below, suggesting that as the target building height increases (larger h_{target}/h_{ave}), the surrounding interference effect decreases (larger $\Delta C_{p_{target}}/\Delta C_{p_{ave}}$). It is possible that with more data to further strengthen the correlation, the target building ΔC_p might be accurately estimated using the local geometric heights of the interfering buildings.

$$\frac{\Delta C_{p_{target}}}{\Delta C_{p_{ave}}} = 1.234\frac{h_{target}}{h_{ave}} - 0.300 \tag{4}$$

Conclusion and Future Work

CFD simulations were performed using OpenFOAM® software using large-eddy simulations of a random urban array. The wind pressure distribution of the random model was analysed for two wind directions to investigate the wind-induced interference effects specifically in random building clusters.

Firstly, the validation was performed for the mean velocity profiles using the previous wind tunnel result. The mean velocity used was averaged for a period of $400T$, which was found to be sufficient for a turbulent flow. The agreement of our results indicated the suitability of the numerical settings applied in this study. Secondly, the contour plots of wind pressure coefficients ($C_{p_{ref}}$) were shown surrounding the tallest building at four different heights. Each height showed different levels of wind-induced interference effects between the clustered buildings. Thirdly, the similar building was used for analysing $C_{p_{ref}}$ distributions along four horizontal sections of varying heights. Both sets of results clearly indicated that as height increased, the level of surrounding interference reduced thereby increasing the $C_{p_{ref}}$ values.

Finally, the ΔC_p based on the pressure difference between windward and leeward building surfaces was obtained for target buildings in all clusters of the two simulation cases. The distribution of the normalized ΔC_p was highly correlated to the normalized target building height as a parameter for the surrounding interference effect. This suggests that the wind-induced interference effects can be potentially parameterized in future work particularly for the accurate estimation of target building C_p.

Acknowledgement

References

[1] J. Hang, Y. Li and M. Sandberg, "Experimental and numerical studies of flows through and within high-rise building arrays and their link to ventilation strategy," *J. Wind Eng Ind Aerod*99, 1036-1055 (2011).

[2] S. A. Zaki, A. Hagishima and J. Tanimoto, "Experimental study of wind-induced ventilation in urban building of cube arrays with various layouts," *J. Wind Eng. Ind. Aerod.*103, 31-40 (2012).

[3] M. Lin, J. Hang, Y. Li, Z. Luo and M. Sandberg, "Quantitative ventilation assessments of idealized urban canopy layers with various urban layouts and the same building packing density," *Build Environ*79, 152-167 (2014).

[4] N. F. M. Kasim, S. A. Zaki, M. S. M. Ali, N. Ikegaya and A. Abd Razak, "Computational study on the influence of different opening position on wind-induced natural ventilation in urban building of cubical array," *Procedia Engineering*169, 256-263 (2016).

[5] A. C. Khanduri, T. Stathopoulos and C. Bédard, "Wind-induced interference effects of building – a review of the state-of-the-art," *Eng Struct* 20 (7), 617-630 (1998).

[6] Y. Li, Q. S. Li and K. L. Ju, "Experimental investigation of the wind pressure distribution and wind interference effects on a typical tall building," *Adv Mat Res*639-640, 444-451 (2013).

[7] A. K. Desai, J. K. Sevalia and S. A. Vasanwala, "Wind interference effect on tall building," *Int. J. Civil, Environmental, Structural, Construction and Architectural Eng.* 8 (6), 656-662 (2014).

[8] J. T. Millward-Hopkins, A. S. Tomlin, L. Ma, D. Ingham and M. Pourkashanian, "Estimating aerodynamic parameters of urban-like surfaces with heterogeneous building heights," *Bound-Lay Meteorol*141 (3), 443-465 (2011).

[9] S. A. Zaki, A. Hagishima, J. Tanimoto and N. Ikegaya, "Aerodynamic parameters of urban building arrays with random geometries," *Bound-Lay Meteorol*138, 99-120 (2011).

[10] S. A. Zaki, A. Hagishima, J. Tanimoto, A. F. Mohammad and A. Abd Razak, "Estimation of aerodynamic parameters of urban building arrays using wind tunnel measurements," *J. Engineering Science and Technology* 9 (2), 176-190 (2014).

[11] A. F. Mohammad, S. A. Zaki, A. Hagishima and M. S. M. Ali, "Determination of aerodynamic parameters of urban surfaces: methods and results revisited," *Theor Appl Climatol*122 (3-4), 635-649 (2014).

[12] V. B. L. Boppana, Z. –T. Xie and I. P. Castro, "Large-eddy simulation of dispersion from surface sources in arrays of obstacles," *Bound-Lay Meteorol*135, 433-454 (2010).

[13] N. Ikegaya, A. Hagishima, J. Tanimoto, Y. Tanaka, K. Narita and S. A. Zaki, "Geometric dependence of the scalar transfer efficiency over rough surfaces," *Bound-Lay Meteorol*143, 357-377 (2012).

[14] M. N. H. A. Razali, S. A. Zaki, M. S. M. Ali and N. Arai, "A numerical analysis of wind flow within and above idealised modified terraced house canyon in Malaysia," *Procedia Engineering*169, 289-296 (2016).

[15] S. A. Zaki, A. Z. Jaafar, A. F. Mohammad, M. S. M. Ali and A. Abd Razak, "Investigation of surface roughness impact on mean wind flow using RNG k-ε model," *Jurnal Teknologi*78 (9), 21-28 (2016).

[16] T. R. Oke, *Boundary Layer Climates*, 2nd ed.(Taylor & Francis,

Vancouver, 1987), pp. 264 – 268.

[17] A. Abd Razak, A. Hagishima, N. Ikegaya, J. Tanimoto, "Analysis of airflow over building arrays for assessment of urban wind environment," *Build Environ*59, 56-65 (2013).

[18] Z.-T. Xie, O. Coceal and I. P. Castro, "Large-eddy simulation of flows over random urban-like obstacles," *Bound-Lay Meteorol*129, 1-23 (2008).

[19] X. Jiang and C. -H. Lai, *Numerical Techniques for Direct and Large-Eddy Simulations* (CRC Press, Boca Raton, 2009), pp. 13 – 19.

[20] Y. C. Kim, A. Yoshida and Y. Tamura, "Characteristics of surface wind pressures on low-rise building located among large group of surrounding buildings," *Eng Struct* 35, 18-28 (2012).